

ไดโอดเปล่งแสงแบบฟิล์มบางในช่วงที่ตามองเห็นชนิดวัสดุอะมอร์ฟัสซิลิคอนอัลลอย
และการประยุกต์ใช้งานในออปโตอิเล็กทรอนิกส์

นายวิโรจน์ บุญโกสุมภ์



วิทยานิพนธ์นี้เป็นส่วนหนึ่งของการศึกษาหลักสูตรปริญญาวิศวกรรมศาสตรดุษฎีบัณฑิต
ภาควิชาวิศวกรรมไฟฟ้า

บัณฑิตวิทยาลัย จุฬาลงกรณ์มหาวิทยาลัย

พ.ศ. 2539

ISBN 974-633-233-3

ลิขสิทธิ์ของบัณฑิตวิทยาลัย จุฬาลงกรณ์มหาวิทยาลัย

**VISIBLE-LIGHT AMORPHOUS SILICON ALLOY
THIN FILM LIGHT EMITTING DIODES
AND THEIR APPLICATIONS IN OPTOELECTRONICS**

MR. WIROTE BOONKOSUM

ศูนย์วิทยทรัพยากร
จุฬาลงกรณ์มหาวิทยาลัย

**A Dissertation Submitted in Partial Fulfillment of the Requirements
for the Degree of Doctor of Engineering
Department of Electrical Engineering
Graduate School
Chulalongkorn University
1996
ISBN 974-633-233-3**

Dissertation Title: Visible-Light Amorphous Silicon Alloy Thin Film Light
Emitting Diodes and Their Applications in Optoelectronics
By: Mr. Wirote Boonkosum
Department of Electrical Engineering
Dissertation Advisors: Assistant Professor Dr. Dusit Kruangam and
Professor Dr. Somsak Panyakeow

Accepted by the Graduate School, Chulalongkorn University in Partial
Fulfillment of the Requirements for the Doctor's Degree.

Santi Thoongsuwan

..... Dean of Graduate School
(Associate Professor Santi Thoongsuwan, Ph. D.)

Dissertation Committee

Yoshihiro Hamakawa

..... Chairman
(Professor Dr. Yoshihiro Hamakawa)

Dusit Kruangam

..... Dissertation Advisor
(Assistant Professor Dr. Dusit Kruangam)

Somsak Panyakeow

..... Co-Dissertation Advisor
(Professor Dr. Somsak Panyakeow)

Virulh Sa-yakanit

..... Member
(Professor Dr. Virulh Sa-yakanit)

Montri Sawadsaringkarn

..... Member
(Associate Professor Dr. Montri Sawadsaringkarn)

Korakot Wattanawichien

..... Member
(Associate Professor Dr. Korakot Wattanawichien)



พิมพ์ต้นฉบับบทคัดย่อวิทยานิพนธ์ภายในกรอบสี่เหลี่ยมนี้เพียงแผ่นเดียว

โรจน์ บุญโกสมภ : ไดโอดเปล่งแสงแบบฟิล์มบางในช่วงที่ตามองเห็นชนิดวัสดุอะมอร์ฟัสซิลิคอนอัลลอยและการประยุกต์ใช้งานในออปโตอิเล็กทรอนิกส์ (VISIBLE-LIGHT AMORPHOUS SILICON ALLOY THIN FILM LIGHT EMITTING DIODES AND THEIR APPLICATIONS IN OPTOELECTRONICS) อ.ที่ปรึกษา : ผศ.ดร.ดุสิต เครืองาม และ ศ.ดร.สมศักดิ์ ปัญญาแก้ว, 195 หน้า . ISBN 974-633-233-3

ได้มีการคิดค้นการออกแบบและประดิษฐ์ไดโอดเปล่งแสงแบบฟิล์มบางชนิดวัสดุอะมอร์ฟัสสารกึ่งตัวนำ ได้สำเร็จเป็นครั้งแรก สิ่งประดิษฐ์มีโครงสร้างเป็นรอยต่อ p-i-n ของฟิล์มบางอะมอร์ฟัสซิลิคอนอัลลอยชนิดที่มีช่องว่างพลังงานกว้างซึ่งได้แก่ อะมอร์ฟัสซิลิคอนไนไตรด์ (a-SiN:H) อะมอร์ฟัสซิลิคอนคาร์ไบด์ (a-SiC:H) และอะมอร์ฟัสซิลิคอนออกไซด์ (a-SiO:H) ฟิล์มบางเหล่านี้เตรียมด้วยวิธี glow discharge plasma CVD ไดโอดเปล่งแสงแบบฟิล์มบางนี้สามารถเปล่งแสงสีต่างๆ ที่ตามองเห็นได้ตั้งแต่สีแดง สีส้ม สีเหลือง สีเขียว ไปจนถึงสีน้ำเงินขาว สีของการเปล่งแสงกำหนดจากขนาดของช่องว่างพลังงานของชั้น i

ในวิทยานิพนธ์นี้ฟิล์ม a-SiN:H, a-SiC:H และ a-SiO:H ถูกนำไปศึกษาคุณสมบัติพื้นฐานต่างๆ อย่างละเอียดและอย่างเป็นระบบทั้งคุณสมบัติทางโครงสร้าง (IR, ESR) คุณสมบัติทางแสง (การดูดกลืนแสง, ช่องว่างพลังงาน, การเปล่งแสงโฟโตลูมิเนสเซนซ์) และคุณสมบัติทางไฟฟ้า (สภาพนำไฟฟ้า) ผลการวิจัยพบว่าระดับพลังงานชนิด localized states ในช่องว่างพลังงานมีอิทธิพลมากต่อคุณสมบัติพื้นฐานของฟิล์ม ข้อมูลที่ได้ในการศึกษาคุณสมบัติพื้นฐานของฟิล์มเหล่านี้มีประโยชน์มากในการนำไปใช้ออกแบบ และประดิษฐ์ไดโอดเปล่งแสงแบบฟิล์มบาง ตลอดจนใช้ในการวิเคราะห์ลักษณะสมบัติต่างๆ ของไดโอดเปล่งแสงแบบฟิล์มบาง

ไดโอดเปล่งแสงแบบฟิล์มบางที่พัฒนาขึ้นสำเร็จในงานวิทยานิพนธ์นี้มีโครงสร้างพื้นฐานประกอบด้วยแผ่นกระจก/ฟิล์มโปร่งแสงที่นำไฟฟ้าได้ (ITO)/ฟิล์มอะมอร์ฟัสซิลิคอนอัลลอยชั้น p-i-n/ฟิล์มขั้วไฟฟ้า Al ไดโอดเปล่งแสงแบบฟิล์มบางนี้เปล่งแสงได้ด้วยหลักการของการฉีดกระแสไฟฟ้า กล่าวคือ ฉีดโฮลจากชั้น p และอิเล็กตรอนจากชั้น n ให้เข้าไปรวมตัวกันในชั้น i ซึ่งเป็นชั้นเปล่งแสง แรงดันไฟฟ้าที่ใช้ไบแอสเพื่อฉีดกระแสไฟฟ้ามีค่าประมาณ 5-15 โวลต์ ความสว่างสูงสุดของแสงที่เปล่งมีค่าอยู่ในช่วง 0.1-1 cd/m² โดยใช้กระแสไฟฟ้าประมาณ 100-1000 mA/cm² นอกจากนี้ได้มีการศึกษาหาความหนาที่เหมาะสมของชั้น i ทั้งทางทฤษฎีและการทดลอง พบว่าความหนาที่เหมาะสมของชั้น i มีค่าประมาณ 500 Å

ในวิทยานิพนธ์ได้มีการเปรียบเทียบคุณสมบัติการเปล่งแสงของไดโอดเปล่งแสงแบบฟิล์มบางที่ชั้น i ผลิตจากวัสดุอะมอร์ฟัสหลายชนิด ผลการวิจัยพบว่า ไดโอดเปล่งแสงแบบฟิล์มบางที่ชั้น i ผลิตจาก a-SiC:H จะเปล่งแสงได้สว่างสูงที่สุด และความสว่างรองลงมาได้แก่ a-SiN:H และ a-SiO:H ตามลำดับ

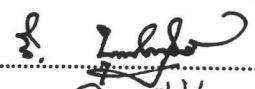
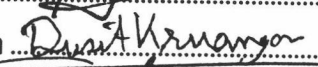
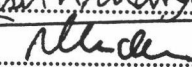
ได้มีความพยายามในการปรับปรุงความสว่างของไดโอดเปล่งแสงแบบฟิล์มบางหลายวิธี ได้แก่ 1) การปรับปรุงประสิทธิภาพของการรวมตัวแบบเปล่งแสงของพาหะ โดยการใช้แผ่นโลหะซึ่งมีคุณสมบัตินำความร้อนได้ดีและสะท้อนแสงได้ดีเป็นแผ่นฐานแทนแผ่นกระจก และ 2) ได้มีการปรับปรุงประสิทธิภาพของการฉีดพาหะ (โฮล) โดยการใช้ฟิล์มอะมอร์ฟัสซิลิคอนออกไซด์ (a-SiO:H) และไมโครคริสตัลไลน์ซิลิคอนออกไซด์ (μc-SiO:H) ชนิด p ซึ่งมีคุณสมบัตินำไฟฟ้าได้ดีและมีช่องว่างพลังงานกว้างเป็นชั้นฉีดโฮลแทน a-SiC:H ชนิด p ทำให้ความสว่างของไดโอดเปล่งแสงแบบฟิล์มบางสูงขึ้นถึงระดับ 10 cd/m²

ในด้านการพัฒนาเป็นดิสเพลย์ ได้ประสบความสำเร็จในการประดิษฐ์ไดโอดเปล่งแสงแบบฟิล์มบางให้เปล่งแสงเป็นรูปร่างลักษณะต่างๆ อีกทั้งผลิตให้มีโครงสร้างเป็นเมตริกซ์และมีพื้นที่กว้างใหญ่ขนาดร้อยตารางเซนติเมตรได้สำเร็จ

ในวิทยานิพนธ์นี้ยังได้ประสบความสำเร็จในการประดิษฐ์โพลีเมอร์ชนิดอะมอร์ฟัสสารกึ่งตัวนำเป็นครั้งแรก คือมีไดโอดเปล่งแสงแบบฟิล์มบางเป็นภาคเปล่งแสงและมีเซลล์แสงอาทิตย์ชนิดอะมอร์ฟัสซิลิคอนเป็นภาครับแสง

ข้อดีเด่นของไดโอดเปล่งแสงแบบฟิล์มบางชนิดอะมอร์ฟัสสารกึ่งตัวนำนี้ ได้แก่ 1) ต้นทุนการผลิตต่ำเพราะใช้วัสดุราคาถูกและผลิตด้วยวิธี CVD ที่อุณหภูมิเพียง 190°C 2) ผลิตเป็นฟิล์มบางพื้นที่ใหญ่ๆ ได้ง่าย ทำให้ได้ดิสเพลย์ขนาดใหญ่ 3) ผลิตบนแผ่นฐานวัสดุชนิดต่างๆ ได้ เช่น แผ่นกระจก แผ่นโลหะ แผ่นพลาสติก แผ่นเซรามิก ทำให้ได้ดิสเพลย์รูปร่างและการใช้งานหลากหลาย เป็นต้น

ภาควิชา วิศวกรรมไฟฟ้า
สาขาวิชา วิศวกรรมไฟฟ้า
ปีการศึกษา 2538

ลายมือชื่อนิสิต 
ลายมือชื่ออาจารย์ที่ปรึกษา 
ลายมือชื่ออาจารย์ที่ปรึกษาร่วม 

C515853 : MAJOR ELECTRICAL ENGINEERING

KEY WORD: : THIN FILM LIGHT EMITTING DIODE / AMORPHOUS SILICON ALLOY / DISPLAY / PHOTOCOUPLER

WIROTE BOONKOSUM : VISIBLE-LIGHT AMORPHOUS SILICON ALLOY THIN FILM LIGHT EMITTING DIODES AND THEIR APPLICATIONS IN OPTOELECTRONICS. THESIS ADVISOR : ASST. PROF. DUSIT KRUANGAM, DR. AND PROF. SOMSAK PANYAKEOW DR. 195 pp. ISBN 974-633-233-3

A novel Thin Film Light Emitting Diode (TFLED) has been developed for the first time. The TFLED has a basic structure of glass/ITO/ p-i-n layers of amorphous silicon alloys/Al. The amorphous silicon alloys employed in this work are wide optical energy gap materials, so-called, hydrogenated amorphous silicon nitride (a-SiN:H), hydrogenated amorphous carbide (a-SiC:H) and hydrogenated amorphous silicon oxide (a-SiO:H). The TFLED can emit the visible light having the colors from red, orange, yellow to green and white-blue depending on the optical energy gap of the i-layer.

A detailed study has been done on the basic properties including structural properties (IR absorption, ESR), optical properties (absorption coefficient, optical energy gap, photoluminescence) and electrical properties (conductivity) of the amorphous films.

The TFLED is a carrier-injection type electroluminescent device. The light output comes from the radiative recombination of holes and electrons injected from the p- and n-layers, respectively, into the i-layer. The typical bias voltage is about 5-15 volt, the injection current density is about 100-1000 mA/cm², giving the brightness of about 0.1~1 cd/m². The theoretical and experimental results show that the optimal thickness of the i-layer is about 500 Å.

A study has been done on the effect of the material used in the i-layer on the performances of the TFLED. The result shows that the TFLED with a-SiC:H as the i-layer gives the highest brightness, while a-SiN:H gives the brightness better than a-SiO:H.

A series of trials has also been done on the improvement of the brightness of the TFLED. The first attempt is to improve the radiative recombination efficiency by using a metal substrate instead of a glass substrate. The metal substrate is good thermal conductive material so that it can dissipate heat from the TFLED to the ambient with better efficiency than a glass substrate. The other attempt is to improve the injection efficiency of holes by using p-type highly-conductive and wide optical energy gap amorphous silicon oxide (p-a-SiO:H) and microcrystalline silicon oxide (p-μc-SiO:H) instead of conventional p-a-SiC:H. The result shows that the brightness was improved to the level of 10 cd/m².

A series of experiments has been done on the fabrication of TFLED displays that can emit light with desired emitting patterns. A new type of dot matrix TFLED display has also been proposed and fabricated for the first time. The screen size for the demonstration is 8 x 8 cm².

In this thesis a new type of amorphous photocoupler having the amorphous TFLED as a light source and the amorphous silicon solar cell as a detector has been developed for the first time.

The advantages of the amorphous TFLED are as follows : 1) low-cost, because the TFLED is made from low-cost amorphous materials and uses a low temperature CVD process (190 °C), 2) it has the possibility to be produced as a large area display, 3) it can be deposited on various substrates, such as glass, metal, plastic, ceramic sheets; therefore various forms of displays can be realized, etc.

ภาควิชา.....Electrical engineering.....

สาขาวิชา.....Electrical engineering.....

ปีการศึกษา..... 2538.....

ลายมือชื่อนิสิต..... *W. Boonkosum*.....

ลายมือชื่ออาจารย์ที่ปรึกษา..... *Dusit Krungam*.....

ลายมือชื่ออาจารย์ที่ปรึกษาร่วม..... *Somsak Panyakeow*.....

Acknowledgments

This work has been done at the Semiconductor Device Research Laboratory (SDRL), Department of Electrical Engineering, Faculty of Engineering, Chulalongkorn University under the supervision of Assistant Professor Dr. Dusit Kruangam and Professor Dr. Somsak Panyakeow.

The author would like to express his greatest acknowledgments to his Supervisor, Assistant Professor Dr. Dusit Kruangam, and to his Co-Supervisor, Professor Dr. Somsak Panyakeow, for providing the author with the opportunity to do this research in the laboratory; their valuable guidance and encouragement throughout the course of this thesis work and also the critical reading this thesis.

The author wishes to make deep acknowledgment to the members of the Dissertation Committee: Professor Dr. Yoshihiro Hamakawa (Osaka University), Professor Dr. Virulh Sa-yakanit (Chulalongkorn University: CU), Professor Dr. Somsak Panyakeow (CU), Associate Professor Dr. Montri Sawadsaringkarn (CU), Associate Professor Dr. Korakot Wattanawichien (Kasetsart University), and Assistant Professor Dr. Dusit Kruangam (CU) for their critical reading, useful discussion and kind guidances.

The author is deeply grateful to Associate Professor Dr. Chatree Sripaipan; the Head of the Department of Electrical Engineering for his encouragement and useful discussions.

The author wishes to make deep acknowledgment to Associate Professor Dr. Banyong Toprasertpong, Associate Professor Dr. Choopol Antarasena, Assistant Professor Dr. Tara Cholapranee, Assistant Professor Dr. Mana Sriyudthsak and Dr. Somchai Ratanathamphan for their kind and useful guidances in the course of this study at SDRL, Department of Electrical Engineering, Faculty of Engineering, Chulalongkorn University.

The author is much indebted to Dr. Bancherd DeLong; visiting scientist from Premier Global Corporation Co. Ltd. for his technical assistance and valuable discussions.

The author wishes to thank Dr. H. Sakai and Dr. S. Fujikake of Fuji Electric R&D Corporation, Japan, for the technical assistance in the preparation of p-type amorphous silicon oxide (a-SiO:H) and p-type microcrystalline amorphous silicon. The author is much indebted to Mr. H. Maehata of Hitachi Zosen Corporation, Japan, for the donation of the stainless steel substrates.

The author is grateful to Mr. Supachok Thainoi, Mrs. Banditha Ratwiset, Mrs. Kwanruan Thainoi, Mr. Prawit Cheewatas, Mr. Anusak Ketsamran, Mr. Preecha Bumampkai for their kind encouragements and skillful technical assistances throughout this thesis work.

The author wishes to express his thanks to the graduate students of SDRL, particularly, Mr. Suwat Sopitpan, Mr. Arporn Teeramongkonrasmee, Miss Thipwan Sujaridchai and Mr. Pavan Siamchai (present address: Tokyo Institute of Technology, Japan) for their kind encouragements and useful discussions.

The author is deeply grateful to the Division of Research, Chulalongkorn University, for supporting the Research Assistance Scholarship to the author throughout this thesis work.

During this thesis work, the author got the financial supports from several organizations for traveling abroad for the presentation of the research achievements. The author would like to express his thanks to the Graduate School of Chulalongkorn University, the Telephone Organization of Thailand, the Alumni Association of Engineering, Chulalongkorn University and the Fellow Program of Department of Electrical Engineering (sponsored by National Science and Technology Development Agency and Chulalongkorn University).

The author is much indebted to the Telephone Organization of Thailand for permitting the author to leave for his Doctor's Degree study at Chulalongkorn University.

Finally, the author wishes to thank his wife, his daughter and his parents for their endless and warm encouragements.

TABLE OF CONTENTS

	Page
Abstract (in Thai).....	IV
Abstract.....	V
Acknowledgements.....	VI
List of Tables.....	XIII
List of Figures.....	XIV
List of Symbols.....	XXV
Chapter 1 Introduction.....	1
1.1 Historical Background.....	1
1.2 Significance of This Work.....	4
1.3 Purpose and Contents of This Work.....	6
References.....	12
Chapter 2 Preparation of Amorphous Silicon Alloys by Glow Discharge Plasma CVD Method.....	16
2.1 Introduction.....	16
2.2 Preparation of Amorphous Silicon Alloys by Glow Discharge Plasma CVD System.....	17
2.2.1 Structure of Glow Discharge Plasma CVD System.....	17
2.2.2 Substrate Preparation.....	19
2.2.3 Film Deposition.....	19
2.3 Summary.....	22
References.....	23
Chapter 3 Development of Amorphous Silicon Alloy Thin Film Light Emitting Diode Having a-SiN:H as a Luminescent Layer.....	25
3.1 Introduction.....	25
3.2 Structural Properties of a-SiN:H Films.....	26

3.2.1 Measurement of Hydrogen Contents in a-SiN:H Film by Infrared Absorption Spectra.....	26
3.2.2 Measurement of Dangling Bond Density in a-SiN:H Films by Electron Spin Resonance (ESR).....	30
3.3 Optical Properties of a-SiN:H Films.....	33
3.3.1 Optical Absorption Edge of a-SiN:H Films.....	33
3.3.2 Photoluminescence (PL) of a-SiN:H Films.....	36
3.3.2.1 Dependence of PL Spectra on Optical Energy Gap.....	38
3.3.2.2 Excitation Energy Dependence of PL Spectra.....	41
3.3.2.3 Effect of External Applied Electric Field on the PL Properties.....	44
3.4 Structure and Fabrication of Thin Film Light Emitting Diode Having a-SiN:H as a Luminescent Layer.....	46
3.4.1 Basic Structure of a-SiN:H TFLED.....	46
3.4.2 Preparation and Characterizations of p- and n-a-SiC:H Films for Carrier Injection Layers.....	48
3.4.3 Fabrication Process of a-SiN:H TFLED.....	51
3.5 Basic Characteristics of a-SiN:H TFLED.....	52
3.5.1 Carrier Injection Mechanism in a-SiN:H TFLED.....	52
3.5.2 Electroluminescent (EL) Spectra.....	56
3.5.3 Relationship Between Brightness and Current Injection Density of a-SiN:H TFLED.....	59
3.5.4 Optimization of Thickness of the i-Layer.....	61
3.5.5 Dependence of EL Intensity on the Frequency-Modulation...	63
3.6 Fabrication of a-SiN:H TFLED Display.....	66
3.6.1 a-SiN:H TFLED with Fixed Emitting Pattern.....	66
3.6.1.1 Determination of Fixed Emitting Pattern by Al Electrodes.....	68

3.6.1.2 Determination of Fixed Emitting Pattern by ITO	
Electrodes.....	73
3.7 Summary.....	73
References.....	75
Chapter 4 Development of Amorphous Silicon Alloy Thin Film Light Emitting Diode Having a-SiC:H as a Luminescent Layer.....	79
4.1 Introduction.....	79
4.2 Preparation of a-SiC:H Films.....	80
4.3 Study of Structural Properties of a-SiC:H Films by IR Absorption and ESR.....	80
4.4 Optical Properties of a-SiC:H Films.....	82
4.4.1 Optical Absorption Edge of a-SiC:H Films.....	82
4.4.2 Photoluminescence (PL) of a-SiC:H Films.....	82
4.5 Structure and Fabrication of Thin Film Light Emitting Diode Having a-SiC:H as a Luminescent Layer.....	85
4.6 Basic Characteristics of a-SiC:H TFLED.....	87
4.6.1 Carrier Injection Mechanism in a-SiC:H TFLED.....	87
4.6.2 Electroluminescent (EL) Spectra.....	89
4.6.3 Relationship Between Brightness and Current Injection Density of a-SiC:H TFLED.....	89
4.6.4 Dependence of EL Intensity on the Frequency-Modulation.....	91
4.7 Fabrication and Demonstrations of a-SiC:H TFLED Displays.....	91
4.8 Summary.....	99
References.....	100
Chapter 5 Development of Amorphous Silicon Alloy Thin Film Light Emitting Diode Having a-SiO:H as a Luminescent Layer.....	103
5.1 Introduction.....	103
5.2 Preparation of a-SiO:H Films.....	104

5.3	Structural Properties of a-SiO:H Films.....	104
5.4	Optical Properties of a-SiO:H Films.....	106
5.4.1	Optical Absorption Edge of a-SiO:H Films.....	106
5.4.2	Photoluminescence (PL) of a-SiO:H Films.....	106
5.5	Structure and Fabrication of Thin Film Light Emitting Diode Having a-SiO:H as a Luminescent Layer.....	108
5.6	Basic Characteristics of a-SiO:H TFLED.....	111
5.6.1	Electrical Properties of a-SiO:H TFLED.....	111
5.6.2	Comparison of Brightness of a-SiN:H, a-SiC:H and a-SiO:H TFLEDs.....	111
5.7	Summary.....	113
	References	114
Chapter 6	Improvement of Brightness of a-SiC:H TFLEDs.....	115
6.1	Introduction.....	115
6.2	Improvement of Brightness by Using Metal-Sheet Substrates.....	116
6.2.1	Advantages of Metal Substrates for Amorphous TFLEDs.....	116
6.2.2	Structure and Fabrication of a-SiC:H TFLED Using Metal Substrate.....	118
6.2.3	Characteristics of a-SiC:H TFLED with Metal Substrate.....	119
6.2.4	Demonstrations of Actual Emissions From a-SiC:H TFLEDs with Metal Substrates.....	126
6.3	Improvement of Brightness by Using Boron doped Highly Conductive and Wide Gap a-SiO:H and $\mu\text{c-SiO:H}$ as p-Layer.....	130
6.3.1	Preparation and Basic Properties of p-a-SiO:H and $\mu\text{c-SiO:H}$ Films.....	130
6.3.2	Fabrication and Characteristics of p-a(μc)-SiO:H/i-a-SiC:H/ n-a-SiC:H TFLED.....	133
6.4	Summary.....	138

References.....	140
Chapter 7 Dot Matrix Amorphous Thin Film Light Emitting Diode Flat Panel Displays.....	142
7.1 Introduction.....	142
7.2 Design and Fabrication of Dot Matrix Amorphous TFLED Displays..	143
7.3 Basic Characteristics of Dot Matrix Amorphous TFLED Displays...	146
7.4 Summary.....	156
References.....	157
Chapter 8 Development of Amorphous Photocoupler Consisting of Amorphous TFLED as a Light Emitting Devices.....	159
8.1 Introduction.....	159
8.2 Development of Amorphous Photocouplers consisting of Amorphous TFLED as a Light Emitting Device.....	162
8.3 Preparation and Device Properties of Amorphous Photocouplers.....	162
8.3.1 Selection of a-SiC:H TFLEDs.....	164
8.3.2 Characteristics of Amorphous Photocouplers.....	166
8.4 Summary.....	172
References.....	173
Chapter 9 Conclusions.....	175
Appendix A Miscellaneous Structures of Amorphous TFLEDs and Amorphous Optoelectronic Integrated Circuits (OE-ICs).....	180
Appendix B Optimization of Thickness of the i-layer.....	183
List of Publications.....	189
Vita.....	194

List of Tables

		page
Table 1.1	Comparison of different types flat panel display devices..... (□ : very good, O : good, Δ : available, X : bad)	2
Table 1.2	Outline of the contribution of the thesis.....	5
Table 2.1	Details of the glow discharge plasma CVD system.....	19
Table 2.2	Typical preparation conditions of the amorphous silicon alloys (a-SiN:H, a-SiC:H and a-SiO:H) by glow discharge plasma CVD method.....	21
Table 3.1	Typical preparation conditions for undoped a-SiN:H.....	26
Table 3.2	Typical preparation conditions of p- and n-type a-SiC:H.....	51
Table 3.3	Typical preparation conditions of a-SiN:H TFLED.....	52
Table 4.1	Typical preparation conditions for undoped a-SiC:H.....	80
Table 4.2	Typical preparation conditions of a-SiC:H TFLED.....	87
Table 5.1	Typical preparation conditions for undoped a-SiO:H by the glow discharge plasma CVD method.....	104
Table 6.1	Thermal conductivity coefficient of glass and various kinds of metals.	124
Table 6.2	Typical preparation conditions for p-a-SiO:H and p-μc-SiO:H.....	131
Table 6.3	Detailed parameters of various structures and various samples of TFLEDs.....	135
Table 7.1	Specifications of 2 versions of the dot matrix a-SiC:H TFLEDs fabricated in the work.....	146
Table 8.1	Examples of the applications of photocoupler.....	160
Table 8.2	Device parameters in amorphous TFLED and amorphous photodiode (TFPD) for the amorphous photocoupler.....	164

List of Figures

	page
Figure 1.1 Optical energy gaps of various amorphous silicon alloys and crystalline semiconductors.....	5
Figure 1.2 Structure of the thesis.....	10
Figure 2.1 Schematic diagram of the glow discharge plasma CVD system.....	18
Figure 2.2 Process of the deposition of amorphous silicon alloy materials by glow discharge plasma CVD method.....	20
Figure 2.3 Photograph of a-SiN:H films deposited on glass substrates.....	21
Figure 3.1 Infrared transmittance spectrum for a-SiN:H film prepared at $\text{NH}_3/(\text{SiH}_4 + \text{NH}_3)$ ratio $x = 0.71$	27
Figure 3.2 Contents of Si-H bonds derived from stretching and wagging modes and content of N-H bonds derived from stretching mode as a function of the ammonia gas fraction x	27
Figure 3.3 Infrared optical absorption coefficient of Si-N, Si-H, and N-H vibrations as a function of the ammonia gas fraction $x = \text{NH}_3/(\text{SiH}_4 + \text{NH}_3)$	29
Figure 3.4 Infrared optical absorption coefficient spectra for undoped a-SiN:H.	29
Figure 3.5 ESR spectrum for undoped a-SiN:H prepared at the ammonia gas fraction $\text{NH}_3/(\text{SiH}_4 + \text{NH}_3) = x = 0.5$	31
Figure 3.6 ESR spin density as a function of the ammonia gas fraction (x).....	31
Figure 3.7 G-value as a function of the ammonia gas fraction (x).....	32
Figure 3.8 Two typical dangling bonds (D.B.) at different sites [6].....	32
Figure 3.9 Optical absorption coefficient spectra near the fundamental band edge for a-SiN:H. The parameter is the ammonia gas fraction $x = \text{NH}_3/(\text{SiH}_4 + \text{NH}_3)$	34
Figure 3.10 Tauc's plot for the determination of the optical energy gap of a-SiN:H.....	34

Figure 3.11	Relationship between the ammonia gas fraction and the optical energy gap of undoped a-SiN:H.....	35
Figure 3.12	Relationship between B value and the ammonia gas fraction (x).....	35
Figure 3.13	Photoluminescent spectra measured at room temperature of undoped a-SiN:H. The parameter is the optical energy gap of undoped a-SiN:H.....	39
Figure 3.14	Dependence of the peak energy of photoluminescent spectra on the optical energy gap for undoped a-SiN:H.....	39
Figure 3.15	Relationship between NH ₃ gas fraction and optical energy gap and PL peak energy for a-SiN:H.....	40
Figure 3.16	Room temperature dependence of the PL spectra on the excitation energy (E _x) for a-SiN:H having the optical energy gap of 2.50 eV...	40
Figure 3.17	Room temperature dependence of the PL peak energy on the excitation energy for various a-SiN:H.....	42
Figure 3.18	Schematic illustrations of (a) the density of states of a-SiN:H and (b) the excitation and recombination processes in a-SiN:H.....	42
Figure 3.19	Photoluminescence of a-SiN:H in case of (a) without biasing electric field and (b) with biasing electric field.....	45
Figure 3.20	Dependence of photoluminescent efficiency on the electric field for a-SiN:H.....	45
Figure 3.21	Basic structures of amorphous TFLED having a-SiN:H as a luminescent layer illustrated in (a) cross section and (b) 3 dimensional view.....	47
Figure 3.22	Band diagrams of p-a-SiC:H/i-a-SiN:H/n-a-SiC:H heterojunction TFLED in (a) thermal equilibrium and (b) forward bias conditions..	47
Figure 3.23	Relationship between the CH ₄ gas fraction and the optical energy gap of a-SiC:H.....	49

Figure 3.24	Dependence of the dark conductivity on the optical energy gap for p-type a-SiC:H.....	49
Figure 3.25	Dependence of the dark conductivity on the reciprocal temperature for p-type a-SiC:H.....	50
Figure 3.26	Fabrication processes of the a-SiN:H TFLED.....	51
Figure 3.27	Room temperature J-V curves for two a-SiN:H TFLEDs. The optical energy gaps of the i-a-SiN:H layer in the upper (red emission) and lower (yellow) TFLEDs are 2.50 eV and 2.90 eV, respectively.....	54
Figure 3.28	Room temperature plot of $\log(J/V^2)$ vs $1/V$ for a red a-SiN:H TFLED.....	54
Figure 3.29	Room temperature EL spectra for two a-SiN:H TFLEDs. The optical energy gaps of the i-a-SiN:H layers are 2.50 eV (red emission) and 2.90 eV (yellow emission).....	57
Figure 3.30	Dependence of the peak energy of EL spectra (E_{EL}) on the NH_3 gas fraction during the preparation of the i-layer.....	57
Figure 3.31	PL spectra excited by various excitation photon energies for undoped a-SiN:H film with the optical energy gap $E_{opt} = 2.50$ eV ...	58
Figure 3.32	Schematic illustration of excitation energy E_x of electron-hole pairs in a-SiN:H.....	58
Figure 3.33	Relationship between the brightness (B) and the injection current density (J) for the red and yellow a-SiN:H TFLEDs.....	60
Figure 3.34	Dependence of the EL intensity on the thickness of the i-a-SiN:H layer for the red TFLEDs.....	60
Figure 3.35	I-V curves of a-SiN:H TFLEDs with different thicknesses of the i-layers.....	62
Figure 3.36	Typical light output waveform response to an input square-wave current pulse for a yellow a-SiN:H TFLED.....	65

Figure 3.37	Dependence of the EL intensity on the modulation frequency in the range of 100 Hz to 1 MHz for a yellow a-SiN:H TFLED.....	65
Figure 3.38	Design rules for fixed emitting patterns of a-SiN:H TFLED.....	67
	(a) The emitting pattern is determined by the pattern of the Al electrode.	
	(b) The emitting pattern is determined by the pattern of the ITO electrode.	
	(c) The emitting pattern is determined by the pattern of the insulating layer inserted in the device.	
Figure 3.39	Photographs of metal masks for the evaporation of Al rear electrodes.....	69
Figure 3.40	Photographs of the a-SiN:H TFLEDs before emitting the light.....	70
Figure 3.41	Photographs of the actual emissions of circle red, yellow, green and white-blue a-SiN:H TFLEDs. The diameter of the circle is 2 mm. The optical energy gaps of the i-a-SiN:H TFLEDs are 2.50, 2.80 and 3.60 eV, respectively. The injection current density is 150 mA/cm ²	70
Figure 3.42	Fabrication process of the ITO electrode with a desired pattern for using in a visible-light amorphous TFLED.....	71
Figure 3.43	Photograph of the actual emission from the a-SiN:H TFLED, (a) before emit the light and (b) during emitting white-blue color light. The emitting pattern of the alphabet “a-SiN” was determined by the ITO electrodes. The height of emitting pattern is 6 mm.....	72
Figure 4.1	ESR spin density of undoped a-SiC:H as a function of carbon gas fraction $x = C_2H_4/(SiH_4+C_2H_4)$	81
Figure 4.2	Relationship between the optical energy gap of undoped a-SiC:H and carbon gas fraction $x = C_2H_4/(SiH_4+C_2H_4)$	81

	page
Figure 4.3 Room temperature PL spectra of undoped a-SiC:H prepared from mixtures of silane and ethylene.....	84
Figure 4.4 Dependences of the PL peak energy and the optical energy gap of a-SiC:H on the carbon gas fraction $x = C_2H_4/(SiH_4+C_2H_4)$	84
Figure 4.5 Schematic illustration of the structure of the a-SiC:H TFLED.....	86
Figure 4.6 Schematic band diagrams of a-SiC:H p-i-n junctions in (a) thermal equilibrium and (b) forward bias conditions.....	86
Figure 4.7 Room temperature I-V curves of a-SiC:H TFLEDs. The parameter is the optical energy gap of the i-layer i.e., 2.60, 2.85 and 3.0 eV, respectively.....	88
Figure 4.8 Room temperature EL spectra of a-SiC:H TFLEDs. The parameter is the optical energy gap of the i-layer i.e., 2.60, 2.85 and 3.0 eV, respectively.....	88
Figure 4.9 Relationship between the brightness of the a-SiC:H TFLED and the injection current density. The parameter E_{opt} is the optical energy gap of the i-layer.....	90
Figure 4.10 Waveforms of the light output response to a square-wave current pulse input for a yellow a-SiC:H TFLED.....	92
Figure 4.11 Dependence of the integral intensity of the light emission from the yellow a-SiC:H TFLED on the frequency of the pulse current.....	92
Figure 4.12 Photographs of various masks used in a photolithography process for etching an ITO electrode.....	94
Figure 4.13 Photographs of several a-SiC:H TFLED displays fabricated in the work.....	94
Figure 4.14 Photograph of an actual emission from a yellowish-orange a-SiC:H TFLED with a rectangular size of $3 \times 5 \text{ mm}^2$. The emitting pattern is determined by the Al rear electrode.....	95

Figure 4.15	Photograph of a yellow color emission from an a-SiC:H TFLED. The emitting pattern is the symbol of the Telephone Organization of Thailand.....	95
Figure 4.16	Photograph of a yellow color emission from an a-SiC:H TFLED. The emitting pattern is "Gear" which is the symbol of the Faculty of Engineering, Chulalongkorn University.....	96
Figure 4.17	Photograph of a yellowish orange color emission from an a-SiC:H TFLED. The emitting pattern is "Cat". The height of the pattern is 2 cm.....	96
Figure 4.18	Photograph of a yellowish orange color emission from an a-SiC:H TFLED. The emitting pattern is "MRS" which is the symbol of the Materials Research Society, U.S.A.....	97
Figure 4.19	Photograph of a yellowish orange color emission from an a-SiC:H TFLED. The emitting pattern is "SSDM" which is the symbol of "Solid State Devices and Materials Conference".....	97
Figure 4.20	Photograph of a yellowish orange color emission from an a-SiC:H TFLED. The emitting pattern is the symbol of "Premier Group of Company".....	98
Figure 5.1	IR absorption spectrum for undoped a-SiO:H prepared at the gas fraction $\text{CO}_2/(\text{SiH}_4+\text{CO}_2) = x = 0.35$	105
Figure 5.2	Relationship between the optical energy gap derived from Tauc's plot and the gas fraction $\text{CO}_2/(\text{SiH}_4+\text{CO}_2)$ for undoped a-SiO:H.....	105
Figure 5.3	Room temperature PL spectra excited by 3250 Å HeCd laser of undoped a-SiO:H.....	107
Figure 5.4	Dependences of the PL peak energy and the optical energy gap on the gas fraction $\text{CO}_2/(\text{SiH}_4+\text{CO}_2)$ for undoped a-SiO:H.....	107
Figure 5.5	Schematic illustration of the structure of an a-SiO:H TFLED.....	109

Figure 5.6	Schematic band diagrams of an a-SiO:H TFLED in (a) thermal equilibrium and (b) forward bias conditions.....	109
Figure 5.7	Room temperature I-V curves of an a-SiO:H TFLED. The parameter is the optical energy gaps of the i-a-SiO:H layer.....	110
Figure 5.8	(a) Structures of three types of amorphous TFLEDs. Sample # 1 has the structure of p-a-SiC:H/ <u>i-a-SiC:H</u> / n-a-SiC:H. Sample # 2 has the structure of p-a-SiC:H/ <u>i-a-SiN:H</u> / n-a-SiC:H. Sample # 3 has the structure of p-a-SiC:H/ <u>i-a-SiO:H</u> / n-a-SiC:H. (b) Comparisons of the brightness of amorphous TFLEDs. The parameter is the i-layers of the amorphous TFLEDs.....	112
Figure 6.1	Example of breaking of a glass substrate due to heat generated in an amorphous TFLED.....	117
Figure 6.2	Schematic illustrations of the structures of the a-SiC:H TFLEDs with (a) glass substrate and (b) metal substrate.....	117
Figure 6.3	Comparison of the I-V curves for the a-SiC:H TFLEDs deposited on stainless steel substrates with different roughness of the surface.	120
Figure 6.4	Comparisons of the brightnesses of a-SiC:H TFLEDs deposited on glass substrates and on SUS substrates.....	120
Figure 6.5	EL spectrum of a-SiC:H TFLED (E_{opt} of i-layer = 3.0 eV) deposited on a SUS substrate.....	121
Figure 6.6	Comparison of the effect of the thickness of the top p-layer on the brightness for the case of the a-SiC:H TFLEDs deposited on SUS substrates.....	121
Figure 6.7	Comparison of dependences of the brightnesses on the electrical power density consumed ($J \times V$) in the TFLEDs deposited on a SUS substrate and on a glass substrate.....	123
Figure 6.8	Schematic illustration of thermal dissipation and back mirror effects in amorphous TFLED deposited on a metal substrate.....	123

Figure 6.9	Relation between the EL intensity and the reciprocal of the measured temperature of TFLEDs. The parameter is the optical energy of the i-layer. The intensity of each TFLED is normalized to the same magnitude at 77 K.....	125
Figure 6.10	Photographs of a-SiC:H TFLEDs deposited on various kinds of metal substrates, e.g., SUS, Cu, Al, Zn.	127
Figure 6.11	Photograph of an actual emission (size 3 x 3 mm ²) from an orange-red a-SiC:H TFLED deposited on a SUS substrate.....	127
Figure 6.12	Photograph of an actual emission (size 3 x 3 mm ²) from a yellow a-SiC:H TFLED deposited on a SUS substrate.....	128
Figure 6.13	Deposition of insulating layers onto specified locations of a metal substrate in advance to the deposition of the p-i-n amorphous layers.....	128
Figure 6.14	Structure of a moving emitting pattern of the a-SiC:H TFLED with a metal substrate.....	129
Figure 6.15	Structure of the a-SiC:H TFLED using a buffer conductive layer before the deposition of p-i-n amorphous layers on a metal substrate.....	129
Figure 6.16	Effect of the CO ₂ /(SiH ₄ +CO ₂) gas fraction on the optical gap, dark conductivity and photoconductivity of p-type μc-SiO:H [11].....	132
Figure 6.17	Photo-and dark conductivity of boron doped a-SiO:H and μc-SiO:H as a function of the optical gap [11].....	132
Figures 6.18	Various structures of the amorphous TFLEDs fabricated in this work.....	134
	(a) glass/ITO/p-a-SiC:H/i-a-SiC:H/n-a-SiC:H/Al.	
	(b) glass/ITO/p-a-SiC:H/i-a-SiN:H/n-a-SiC:H/Al.	
	(c) glass/ITO/p-a-SiC:H/i-a-SiO:H/n-a-SiC:H/Al.	
	(d) glass/ITO/p-a-SiO:H/i-a-SiC:H/n-a-SiC:H/Al.	

(e) glass/ITO/p- μ c-SiO:H/i-a-SiC:H/n-a-SiC:H/Al.

Figure 6.19	EL spectra for a-SiC:H TFLEDs having different p-layers.....	136
Figure 6.20	Dependence of the peak energy of the EL spectrum on the optical energy gaps of the p-layer.....	136
Figure 6.21	Band diagrams of the amorphous TFLED at the vicinity of p/i interface with different optical energy gap of the p-layer.....	137
Figure 6.22	Comparison of the brightnesses of the a-SiC:H TFLEDs which have different materials of the p-layers.....	137
Figure 7.1	Structure of the dot matrix TFLED display.....	144
Figure 7.2	Fabrication process of the dot matrix TFLED display.....	144
Figure 7.3	Photolithography and lift-off techniques for Al grid electrodes.....	145
Figure 7.4	Photographs of the actual emissions from the dot matrix TFLED displays version No.1.....	147
Figure 7.5	Photographs of the actual emissions from the dot matrix TFLED displays version No.2.....	148
Figure 7.6	Photographs of the dot matrix TFLED displays of some selected emitting pixels.....	149
Figure 7.7	Schematic illustration of top view of a dot matrix TFLED display...	150
Figure 7.8	Equivalent circuit of a dot matrix TFLED display.....	150
Figure 7.9	Schematic diagrams of ITO and Al grid electrodes connected by the conductive lateral p- and n-a-SiC:H layers.....	151
Figure 7.10	Equivalent circuit of a dot matrix amorphous TFLED display indicating series lateral resistances between the two adjacent electrodes.....	153
Figure 7.11	Calculated result of the relationship between the magnitude of the leakage current and the spacing distance of ITO electrodes in a dot matrix amorphous TFLED display. The parameter is the conductivity of the p-a-SiC:H layer.....	153

Figure 7.12	Examples of the packages of the dot matrix amorphous TFLED display.....	154
Figure 7.13	Design of a high resolution dot matrix amorphous TFLED display with a pixel area of $0.3 \times 0.3 \text{ mm}^2$ and spacing distance of 0.3 mm.....	155
Figure 8.1	Structures of novel amorphous silicon alloy photocouplers,..... (a) photo-interrupter type having a-Si:H photodiode as a detector, (b) photo-interrupter type having an a-Si:H photoresistor as a detector, (c) photo-isolator type having a-Si:H photodiode as a detector and (d) photo-isolator type having an a-Si:H photoresistor as a detector.	161
Figure 8.2	Examples of encapsulations of amorphous photocouplers.....	163
Figure 8.3	Comparison of a spectral response of an a-Si:H solar cell and emitting spectra of three a-SiC:H TFLEDs in which the optical energy gaps of the i-a-SiC:H layers are 2.6, 2.8 and 3.0 eV, respectively.....	163
Figure 8.4	Output waveforms of a yellow a-SiC:H TFLED driven by pulse current of the frequency from 500 Hz to 20 kHz (duty cycle = 50 %)......	165
Figure 8.5	Dependence of the integral intensity of the light emission from an a-SiC:H TFLED on the frequency of the pulse current source.....	165
Figure 8.6	Relationship between the injection current density (J_{inj}) of an a-SiC:H TFLED (area = $3 \times 5 \text{ mm}^2$) and the short circuit current output (J_{sc}) of an a-Si:H solar cell (area = $3 \times 5 \text{ mm}^2$) constructed in the photo-interrupter type (a).....	167

Figure 8.7	Dependence of the J_{sc} of an a-Si:H solar cell (photodiode) on the distance between the a-SiC:H TFLED and the solar cell. The solid line is a calculated result from the relation of light intensity $\propto 1/(\text{distance})^2$	167
Figure 8.8	Relationship between the input and output signals of the photo-isolator type (c).....	169
Figure 8.9	Relationship between the applied voltage and photocurrent output of the photoresistor in the photo-interrupter type (b).....	169
Figure 8.10	Photograph of the amorphous photocouplers in which the TFLED and the TFPD were deposited on the separated glass substrates.....	170
Figure 8.11	Photograph of the amorphous photoisolator in which the TFLED and the TFPD were deposited on the dual surfaces of a common glass substrate.....	170
Figure 8.12	Examples of the packages of the amorphous photointerrupter and the amorphous photoisolator produced in the work.....	171
Figure A.1	Structure of multi-color amorphous TFLEDs.....	180
Figure A.2	Structures of dual surfaces of amorphous TFLED.....	181
Figure A.3	Illustration of the structure of p-i-n/p-i-n tandem amorphous TFLEDs.....	181
Figure A.4	Example of the combination TFLEDs and TFPDs (thin film photodiode) for utilizations in a novel optoelectronic functional devices.....	182
Figure A.5	Example of the spacial optical connection of multi-layer structures using amorphous TFLEDs & TFPDs.....	182
Figure B.1	Schematic illustrations of band diagrams of a-SiN:H p-i-n junction in thermal equilibrium (a) and in forward bias (b) conditions.....	184
Figure B.2	Illustration of the distribution of the tail states for the i-layer used in the analysis of the electroluminescent properties of TFLEDs [5].	184

List of Symbols

CVD	: Chemical Vapor Deposition
a-SiN:H	: Hydrogenated amorphous silicon nitride
a-SiC:H	: Hydrogenated amorphous silicon carbide
a-SiO:H	: Hydrogenated amorphous silicon oxide
ITO	: Indium Tin Oxide
RF power	: Radio frequency power (13.56 MHz)
SiH ₄	: Silane gas
NH ₃	: Ammonia gas
CH ₄	: Methane gas
C ₂ H ₄	: Ethylene gas
B ₂ H ₆	: Diborane gas
PH ₃	: Phosphine gas
CO ₂	: Carbon dioxide gas
N ₂	: Nitrogen gas
H ₂	: Hydrogen gas
Ar	: Argon gas
LED	: Light Emitting Diode
TFLED	: Thin Film Light Emitting Diode
E _{opt}	: Optical energy gap
E _c	: Conduction band edge
E _v	: Valence band edge
E _F	: Fermi level
EB	: Electron Beam
IC	: Integrated Circuit
TFT	: Thin Film Transistor
LCD	: Liquid Crystal Display

IR	: Infrared	
α	: Optical absorption coefficient	(1/cm)
ω	: Angular frequency	(1/s)
k	: Wave number	(1/cm)
σ	: Electrical conductivity	(S/cm)
n	: Refractive index	
c	: Velocity of light	
E	: Electric field	(V/cm)
h	: Planck's constant	(J.s)
ESR	: Electron Spin Resonance	
DPPH	: Diphenyl Picryl Hydrazyl	
n	: Carrier density	(1/cm ³)
e	: Electronic charge	(C)
K	: Boltzman's constant	(J/K)
T	: Absolute temperature	(K)
σ_D	: Dark conductivity	(S/cm)
T _s	: Substrate temperature	(°C)
h ν	: Photon energy	(eV)
J	: Current density	(A/cm ²)
τ	: Life time of carrier	(s)
λ	: Wave length	
PL	: Photoluminescence	
EL	: Electroluminescence	
E _{opt}	: Optical energy gap	(eV)
ΔE_c	: Conduction band discontinuity	(eV)
ΔE_v	: Valence band discontinuity	(eV)
ϕ_B	: Barrier height for tunneling	(eV)
d	: i-layer thickness	(Å)
V	: Applied voltage	(V)

$n(x)$: Electron density at position x	($1/\text{cm}^3$)
$p(x)$: Hole density at position x	($1/\text{cm}^3$)
B	: Brightness	(cd/m^2)
m_e^*	: Effective mass of electron	
m_h^*	: Effective mass of hole	
γ_p	: Hole range	(μm)
μ_n	: Electron mobility	($\text{cm}^2/\text{V}\cdot\text{s}$)
μ_p	: Hole mobility	($\text{cm}^2/\text{V}\cdot\text{s}$)
τ_p	: Nonradiative recombination life time of holes	(s)
α_c	: Dispersive parameter of electron	
α_v	: Dispersive parameter of hole	
E_X	: Excitation energy	(eV)
E_{EL}	: Peak energy of EL spectra	(eV)
E_{PL}	: Peak energy of PL spectra	(eV)
m^*	: Effective mass of free electron	(kg)
q	: Charge of free electron	(C)
J_n	: Current density based on electrons	(A/cm^2)
J_p	: Current density based on holes	(A/cm^2)
x	: Position in the i-layer	(μm)
d_{max}	: Optimal i-layer thickness	(\AA)
f_c	: Cut-off frequency	(Hz)
I_{leak}	: Leakage current in dot matrix TFLED	(mA)
σ	: Conductivity of p-layer	(S/cm)
d	: Thickness of p-layer	(\AA)
V	: Potential drop between adjacent ITO electrodes	(V)
s	: Spacing distance of ITO electrodes	(μm)

1 : Lenght of ITO electrode (cm)



ศูนย์วิทยทรัพยากร
จุฬาลงกรณ์มหาวิทยาลัย